PSFC/RR-83-01

CCAN and TCAN – $1\frac{1}{2}$-D Compressible-Flow and Time-Dependent Codes for Conductor Analysis

P.J.Gierszewski, A.S.Wan, T.F.Yang

M.I.T.

ABSTRACT

This report documents the computer programs CCAN (steady-state Compressible flow Conductor ANalysis) and TCAN (Time-dependent incompressible-flow Conductor ANalysis). These codes calculate temperature, pressure, power and other engineering quantities along the length of an actively-cooled electrical conductor. Present versions contain detailed property information for copper and aluminum conductors; and gaseous helium, liquid nitrogen and water coolants. CCAN and TCAN are available on the NMFECC CDC 7600.

List of Variables

A	– area (m^2)
B	– magnetic field strength (Tesla)
c	– specific heat at constant pressure (J/kg-K)
D	– hydraulic diameter, $D = 4A_c/P_w$ (m)
D_{coil}	– coil external diameter (m)
f	– Moody friction factor
g	– gravitational acceleration, g = 9.8 m/s^2
G	– mass flux, $G = \rho_c v$ (kg/m^2-s)
h	– surface heat transfer coefficient (W/m^2-K)
h_c	– coolant enthalpy (J/kg)
j	– current density (A/m^2)
k	– thermal conductivity (W/m-K)
K_c	– coolant compressibility (1/Pa)
L	– length (m)
L_m	– radial thermal conduction path length in conductor (m)
Nu	– Nusselt number, $Nu = hD/k_c$
p	– coolant pressure (Pa)
Pr	– Prandtl number, $Pr = \mu_c c_c/k_c$
P_h	– heated perimeter (m)
P_w	– wetted perimeter (m)
P_{elec}	– electrical power (W)
P_{heat}	– external heat input power (W)
P_{pump}	– pump power (W)
P_{refr}	– refrigerator power (W)
r	– radial coordinate (m)
Re	– Reynolds number, $Re = \rho_c v D/\mu_c$
RRR	– residual resistance ratio, $RRR = \eta_{273K}/\eta_{0K}$

List of Variables continued

t	– time (s)
T	– temperature (K)
T_r	– reference temperature for refrigeration cycle (300 K)
$\overline{T}_c$	– mean coolant temperature (K)
v	– coolant velocity (m/s)
V_m	– conductor volume (m^3)
x	– axial coordinate (m)
β_c	– coolant thermal expansivity (1/K)
Δt	– time step size (s)
ΔT_{max}	– maximum magnet temperature rise (K)
$\overline{\Delta T}$	– average magnet temperature rise (K)
Δx	– axial node length (m)
ϵ_{pump}	– pump hydraulic efficiency
ϵ_{refr}	– refrigerator non-Carnot efficiency
η	– electrical resistivity ($\Omega \cdot$ m)
θ	– conductor angle from vertical
τ_s	– wall or surface shear stress (N/m^2)
ρ	– density (kg/m^3)
ψ_c	– coolant Joule-Thompson coefficient (m^2-K/J)

subscripts/superscripts

c	– coolant
j	– adjacent axial node
m	– magnet or, more generally, conductor
n	– axial node
s	– surface
t	– current time step
$t - \Delta t$	– previous time step
tr	– transverse heat conduction

CCAN and TCAN – $1\frac{1}{2}$-D Compressible-Flow and Time-Dependent Codes for Conductor Analysis

P.J.Gierszewski, A.S.Wan, T.F.Yang

This report describes the computer programs CCAN (steady-state Compressible Conductor ANalysis) and TCAN (Time-dependent incompressible flow Conductor ANalysis). These codes calculate temperature, pressure, power and other engineering quantities along the length of an actively cooled electrical conductor. They were developed to perform engineering analyses of internally-cooled conductors for non-superconducting magnets. Present versions contain detailed property information for copper and aluminum conductors; and gaseous helium, liquid nitrogen and water coolants.

The primary assumptions are:

1) Single phase flow;
2) Axial thermal conduction is small relative to heat transferred to coolant;
3) Conductor surfaces not in contact with coolant are adiabatic.

Section 1 reviews the general theory; Sections 2 and 3 describe the analysis used in CCAN and TCAN, respectively; Section 4 the present data base; Section 5 summarizes some validation runs; and Section 6 describes the input (similar for both programs).

1.0 General Theory

This analysis is restricted to single-phase, one-dimensional, constant area flow. It does include time-dependent heat sources, axial property variations, and compressible flow. The latter is required in general because of the large property variations possible at cryogenic temperatures with modest temperature changes (especially for gaseous coolants). The resulting equations do not lend themselves to analytic solution, but under the above assumptions with the additional neglect of azimuthal property variation, a simple marching procedure is adequate with straightforward differencing at each axial zone into coolant, conductor surface and conductor bulk nodes. Care must be taken to avoid choked flow and possible flow instabilities, critical heat flux with liquid coolants, and potential thermal runaway where resistivity changes rapidly with temperature.

In addition to the above assumptions, we neglect axial thermal conduction with respect to radial thermal conduction and consider only an average axial velocity, v. Then, for the coolant, conservation of mass becomes [1]

$$\frac{\partial \rho_c}{\partial t} + \frac{\partial}{\partial x}(\rho_c v) = \frac{\partial \rho_c}{\partial t} + \frac{\partial G}{\partial x} = 0 \tag{1}$$

where $G = \rho_c v$ is the mass flux, ρ_c the coolant density. The momentum equation with conservation of mass is [1]

$$\frac{\partial G}{\partial t} + \frac{\partial}{\partial x}\left(\frac{G^2}{\rho_c}\right) + \frac{\partial p}{\partial x} + \frac{\tau_s P_w}{A_c} + \rho_c g \cos\theta = 0 \tag{2}$$

where p is pressure, τ_s is shear stress at the surface, x is the axial coordinate, P_w is the wetted perimeter, A_c is the coolant cross-sectional area, g gravitational acceleration and θ is the conductor orientation angle clockwise from vertical. Expressing the wall shear in terms of a conventional friction factor f and the hydraulic diameter D, and rearranging,

$$\frac{\partial G}{\partial t} + \frac{\partial p}{\partial x} = -\frac{f}{D}\frac{G^2}{2\rho_c} - \rho_c g \cos\theta - \frac{1}{\rho_c}\frac{\partial}{\partial x}\left(\frac{G^2}{\rho_c}\right) \tag{3}$$

The coolant energy equation with no internal heat sources is, [1]

$$\left(\rho_c \frac{\partial}{\partial t} + G\frac{\partial}{\partial x}\right)\left(h_c + \frac{G^2}{2\rho_c^2}\right) - \frac{q'' P_h}{A_c} + Gg\cos\theta - \frac{\partial p}{\partial t} = 0 \tag{4}$$

where h_c is coolant enthalpy, q'' is the heat flux from conductor to coolant, and P_h is the heated perimeter.

The conductor equations are obtained from the cylindrical heat conduction equation, neglecting axial conduction and radial variation in thermal conductivity,

$$\frac{1}{r}\frac{\partial}{\partial r}\left(r\frac{\partial T_m}{\partial r}\right) + \frac{q'''}{k_m} = \frac{1}{\rho_m c_m k_m}\frac{\partial T_m}{\partial t} \tag{5}$$

where r is radius, T_m is magnet temperature, q''' is volumetric heat source, ρ_m is magnet density, c_m is magnet specific heat and k_m is thermal conductivity.

Finally, the constitutive relations and empirical correlations [2] are

$$q''' = \eta_m j^2 + q'''_{ext} \tag{6}$$

$$q'' = h\left(T_{m,surface} - T_c\right) = q'''\frac{A_m}{P_h} \tag{7}$$

$$Nu = \frac{hD}{k_c} = 0.023 Pr^{0.4} Re^{0.8} \left[1 + 3.5 \frac{D}{D_{coil}} \right] \tag{8}$$

$$f = \frac{0.316}{Re^{0.25}} \left(Re \frac{D^2}{D_{coil}^2} \right)^{0.05} \tag{9}$$

In the above relations, η_m is the conductor electrical resistivity (evaluated at T_m); j is the current density in the conductor; q'''_{ext} is any external volumetric heat source; h is the heat transfer coefficient; Re, Nu and Pr are the usual Reynolds number (evaluated at film conditions in the Nu correlation), Nusselt number and Prandtl number, respectively, and the D/D_{coil} term is a curved pipe correction where D_{coil} is the mean coil external diameter or, equivalently, twice the coil radius of curvature.

The codes also calculate total electrical power P_{elec}, mechanical pump power P_{pump}, external heat input P_{heat} and refrigerator power P_{refr}, in addition to the basic temperature and flow information,

$$P_{elec} = \int_0^L \eta_m j^2 A_m dx \tag{10}$$

$$P_{pump} = \frac{1}{\epsilon_{pump}} \int_0^L \frac{G A_c}{\rho_c} dp \tag{11}$$

$$P_{heat} = \int_0^L q'''_{ext} A_m dx \tag{12}$$

$$P_{refr} = \frac{(P_{pump} + P_{elec} + P_{heat})}{\epsilon_{refr}} \left(\frac{T_r}{\overline{T_c}} - 1 \right) \tag{13}$$

A pump hydraulic efficiency factor ϵ_{pump} is included in the mechanical power expression, Eqn.(11), to allow for incomplete conversion of input electrical power to hydraulic pressure head. The remainder is wasted as heat and can be a significant heat source at cryogenic conditions. A reasonable value for room-temperature mechanical pumps is 70% [7]. Also, the design goal for the ISABELLE ℓHe (liquid helium) cold compressors is 70% isentropic efficiency [4].

Refrigeration power is estimated from a simple Carnot-type formula, Eqn.(13), where $P_{pump} + P_{elec} + P_{heat}$ is the total thermal power to be removed; $(T_r/\overline{T_c} - 1)$ is the Carnot

"ideal refrigerator" factor, T_r is the reference heat sink condition (say, atmosphere at 300 K); $\overline{T_c}$ is an average refrigeration temperature; and ϵ_{refr} is the actual non-Carnot refrigerator efficiency. Typical data on refrigerator efficiencies show more of a relationship of ϵ_{refr} with capacity than with temperature, and $\epsilon_{refr} \approx 0.2 - 0.30$ is typical for kW- to MW-rated units [5,6]. Since the refrigerator removes heat from the coolant over a temperature range $T_{c,max}$ to $T_{c,min}$ in the refrigerator, an average value $\overline{T_c}$ is used in the Carnot efficiency factor, where

$$\frac{1}{\overline{T_c}} = \frac{1}{T_{c,max} - T_{c,min}} \int_{T_{c,min}}^{T_{c,max}} \frac{dT}{T_c} = \frac{\ln(T_{c,max}/T_{c,min})}{T_{c,max} - T_{c,min}} \tag{14}$$

2.0 CCAN – Compressible-Flow Conductor Analysis

CCAN is limited, in addition to the approximations given in Section 1, to steady-state but compressible flow. Taking $\partial/\partial t = 0$ in Eqns. (1) to (5), we obtain

$$\frac{dG}{dx} = 0 \tag{15}$$

$$\frac{dp}{dx} = -\frac{f}{D}\frac{G^2}{2\rho_c} - \rho_c g \cos\theta + \frac{G^2}{\rho_c^2}\frac{d\rho_c}{dx} \tag{16}$$

$$G\frac{dh_c}{dx} - \frac{G^3}{\rho_c^3}\frac{d\rho_c}{dx} - \frac{q''P_h}{A_c} + Gg\cos\theta = 0 \tag{17}$$

$$\frac{1}{r}\frac{d}{dr}\left(r\frac{dT_m}{dr}\right) = -\frac{q'''}{k_m} \tag{18}$$

We wish to determine $p(x)$, $T_c(x)$ and $T_m(x)$. Other variables such as ρ_c and h_c are in general functions of p and T_c. So

$$\frac{d\rho_c}{dx} = \left.\frac{\partial\rho_c}{\partial p}\right|_T \frac{dp}{dx} + \left.\frac{\partial\rho_c}{\partial T_c}\right|_p \frac{dT_c}{dx} \tag{19}$$

and similarly for (dh_c/dx). Making these expansions, substituting into the momentum and energy equations, and making use of the definitions of coolant compressibility K_c, thermal

expansivity β_c, specific heat at constant pressure c_c, and Joule-Thompson coefficient ψ_c:

$$K_c = \frac{1}{\rho_c}\frac{\partial \rho_c}{\partial p}\bigg|_T \tag{20}$$

$$\beta_c = -\frac{1}{\rho_c}\frac{\partial \rho_c}{\partial T_c}\bigg|_p \tag{21}$$

$$c_c = \frac{\partial h_c}{\partial T_c}\bigg|_p \tag{22}$$

$$\psi_c = -\frac{1}{c_c}\frac{\partial h_c}{\partial p}\bigg|_T = \frac{\partial T_c}{\partial p}\bigg|_h = -\frac{1}{\rho_c c_c}(1 - T_c\beta_c) \tag{23}$$

we finally obtain, where all quantities refer to fluid properties,

$$\frac{dT_c}{dx} = \frac{1}{C}\left[\frac{4q''}{GDc_c} + \frac{K_c G^2}{\rho_c c_c}\left(\frac{4q''}{GD} + \frac{fG^2}{D2\rho_c^2}\right) - \psi_c\rho_c\left(\frac{fG^2}{D2\rho_c^2} + g\cos\theta\right) - \frac{g\cos\theta}{c_c}\right] \tag{24}$$

$$\frac{dp}{dx} = \frac{1}{C}\left[-\frac{\beta_c G^2}{\rho_c c_c}\left(\frac{4q''}{GD} + \frac{fG^2}{D2\rho_c^2}\right) - \rho_c\left(\frac{fG^2}{D2\rho_c^2} + \frac{g\cos\theta}{c_c}\right)\right] \tag{25}$$

where

$$C = 1 + \frac{\beta_c G^2}{\rho_c c_c}\left[\frac{1}{\rho_c} + \psi_c c_c - \frac{K_c c_c}{\beta_c}\right] \tag{26}$$

Note that choked flow occurs when C goes to zero. Using the constitutive relations and property data, we can solve for $p(x)$, $T_c(x)$ and all the desired coolant quantities.

Applying an adiabatic outer boundary condition, we obtain, for an internal coolant channel,

$$\Delta T_{max} = \frac{q'''}{4\pi k_m}\left[(A_m + A_c)\ln\left(\frac{A_c + A_m}{A_c}\right) - A_m\right] \tag{27a}$$

$$\overline{\Delta T} = \frac{q'''}{8\pi k_m}\left[\frac{2(A_m + A_c)^2}{A_m}\ln\left(\frac{A_m + A_c}{A_c}\right) - 3A_m - 2A_c\right] \tag{27b}$$

and for an external coolant annulus (i.e., coolant in a ring outside a central solid conductor),

$$\Delta T_{max} = \frac{q''' A_m}{4\pi k_m} \tag{28a}$$

$$\overline{\Delta T} = \frac{q''' A_m}{8\pi k_m} \tag{28b}$$

where ΔT_{max} is the magnet temperature rise from the inner cooled surface to the outer surface, $\overline{\Delta T}$ is the average magnet temperature rise, and the result has been expressed in terms of coolant cross-sectional area A_c and magnet area A_m.

3.0 TCAN – Time-Dependent Conductor Analysis

TCAN calculates time-varying temperature, pressure, power and other quantities along an axially cooled conductor, allowing variable current and inlet temperature, with an incompressible single-phase coolant. It is a modified version of TACC [3]. As in CCAN, the conductor is divided into axial zones, and each zone contains three lumped nodes representing bulk coolant, conductor/coolant interface and bulk conductor. Because of the explicit time and axial dependencies in the resulting equations, the heat transfer and pressure drop equations are written as finite difference equations and solved, for each time step, by marching from inlet to exit.

The general formulae are as in Section 1. We retain time-dependence but assume incompressible flow ($\rho_c =$ constant). We also assume a pump-related boundary condition – constant inlet mass flow rate or $(\partial G/\partial t)_{inlet} = 0$. But then $\partial G/\partial x = 0$ since ρ_c is constant, so G is also fixed. The resulting equations are:

$$G(x,t) = G_0 \tag{29}$$

$$\frac{\partial p}{\partial x} + \frac{f}{D}\frac{G^2}{2\rho_c} + \rho_c g \cos\theta = 0 \tag{30}$$

$$\rho_c \frac{\partial h_c}{\partial t} + G\frac{\partial h_c}{\partial x} - \frac{q'' P_h}{A_c} + Gg\cos\theta = 0 \tag{31}$$

$$\frac{k_m}{r}\frac{\partial}{\partial r}\left(r\frac{\partial T_m}{\partial r}\right) + q''' = \frac{1}{\rho_m c_m}\frac{\partial T_m}{\partial t} \tag{32}$$

In the actual implementation of these equations, properties are evaluated at the most recent time or axial node conditions, and ρ_c in particular may change. Consequently, the incompressibility assumption is relaxed somewhat and replaced by the assumption

that the compressibility terms in the fluid equations can be neglected with respect to the other terms. Furthermore, the compressibility-related term $(\partial\rho_c/\partial x)G^2/\rho_c^3$ in the pressure equation is retained to improve prediction of choked flow conditions.

As in the CCAN analysis, $\rho_c = \rho_c(p,T)$ and $h_c = h_c(p,T)$. In general, $dh_c = -c_c\psi_c dp + c_c dT_c$ where ψ_c is the Joule-Thompson coefficient. We neglect ψ_c in TCAN since situations where the Joule-Thompson effect matters usually require full compressible flow analysis anyway (e.g. gaseous helium below 10 K), so $dh_c = c_c dT_c$ and the energy equation simplifies to

$$\rho_c c_c \frac{\partial T_c}{\partial t} + G c_c \frac{\partial T_c}{\partial x} - \frac{q'' P_h}{A_c} + Gg\cos\theta = 0 \tag{33}$$

Eqns.(30),(32) and (33) are written in a partially implicit finite difference form as:

Coolant momentum equation (node $n+1$ at time step t):

$$\frac{p^t_{n+1} - p^t_n}{\Delta x} + \frac{f^{t-\Delta t}}{D}\frac{G^2}{2\rho_c} + \rho_c g\cos\theta - \left[\frac{\Delta\rho_c}{\Delta x}\frac{G^2}{\rho_c^3}\right]^{t-\Delta t} = 0 \tag{34}$$

Coolant energy equation (node $n+1$ at time t):

$$\rho_c c_c\left(\frac{T^t_{c,n+1} - T^{t-\Delta t}_{c,n+1}}{\Delta t}\right) + \frac{G c_c}{\Delta x}\left(\frac{T^t_{c,n+1} + T^{t-\Delta t}_{c,n+1}}{2} - \frac{T^t_{c,n} + T^{t-\Delta t}_{c,n}}{2}\right)$$

$$-\frac{hP_h}{A_c}\left(T^t_{s,n} - T^t_{c,n+1}\right) + Gg\cos\theta = 0 \tag{35}$$

Conductor bulk energy equation (node n at time step t):

$$-\frac{P_h \Delta x k_m}{L_m}\left(T^t_{m,n} - T^t_{s,n}\right) - h_{tr}A_{tr}\left(T^{t-\Delta t}_{m,n} - T^{t-\Delta t}_{m,j}\right)$$

$$+A_m\Delta x\left(\frac{q^t + q^{t-\Delta t}}{2}\right) = \frac{A_m \Delta x}{\rho_m c_m}\left(\frac{T^t_{m,n} - T^{t-\Delta t}_{m,n}}{\Delta t}\right) \tag{36}$$

Interface temperature equation (node n at time t):

$$\frac{k_m}{L_m}\left(T^t_{m,n} - T^t_{s,n}\right) = h\left(T^t_{s,n} - T^t_{c,n+1}\right) \tag{37}$$

where the superscript denotes the time step; subscripts c, m and s indicate coolant, magnet (conductor) and surface (interface) values; subscripts n, $n+1$ and j denote axial

node; q is an external volumetric heat source; L_m is an effective thermal conduction path length between the conductor bulk temperature node and the interface temperature node; and $h_{tr}A_{tr}$ is an effective heat transfer coefficient and area for heat transfer between axial nodes n and j.

In these difference equations, coolant node 1 is the inlet, so coolant node 2 is the first axial node actually in the conductor and corresponds to conductor node 1. The variables are referred to time steps t or $t-\Delta t$ so as to make the most important variables implicit and other terms estimated explicitly from previous time step values. As a result of this differencing, the equations can be solved directly for $T^t_{c,n+1}$, $T^t_{s,n}$, $T^t_{m,n}$ and p^t_{n+1} in terms of known previous time step and axial node values, yielding:

$$T^t_{c,n+1} = C_1C_2\left(\frac{k_mP_h\Delta x\Delta t}{L_m(1+k_r)}\right)\left[A_m\Delta x\Delta t\bar{q} + A_m\Delta x\rho_m c_m T^{t-\Delta t}_{m,n} - h_{tr}A_{tr}\Delta t(T^{t-\Delta t}_{m,n} - T^{t-\Delta t}_{m,j})\right]$$

$$+C_1\left[\frac{GA_cc_c\Delta t}{2}\left(T^t_{c,n} + T^{t-\Delta t}_{c,n} - T^{t-\Delta t}_{c,n+1}\right) + A_m\Delta x\rho_m c_m - A_c\Delta x\Delta t G g\cos\theta\right] \tag{38}$$

$$T^t_{m,n} = C_2\left[A_m\Delta x\Delta t q + A_m\Delta x\rho_m c_m T^{t-\Delta t}_{m,n}\right.$$

$$\left.+\frac{k_mP_h\Delta x\Delta t}{L_m(1+k_r)}T^t_{c,n+1} - h_{tr}A_{tr}\Delta t\left(T^{t-\Delta t}_{m,n} - T^{t-\Delta t}_{m,j}\right)\right] \tag{39}$$

$$T^t_{s,n} = \frac{T^t_{c,n+1} + k_rT^t_{m,n}}{1+k_r} \tag{40}$$

$$p^t_{n+1} = p^t_n - \frac{f^{t-\Delta t}}{D}\frac{G^2}{2\rho_c} - \rho_c g\cos\theta + \left[\frac{\Delta\rho_c}{\Delta x}\frac{G^2}{\rho_c^3}\right]^{t-\Delta t} \tag{41}$$

where $k_r = k_m/hL_m$; $L_m \simeq (\sqrt{A_m + A_c} - \sqrt{A_c})/2\sqrt{\pi}$ is the approximate radial conduction length with internal cooling, and $L_m \simeq \sqrt{A_m/\pi}/2$ is the average radial length for solid conductors with external cooling; $\bar{q} = (q^t - q^{t-\Delta t})/2$; and

$$\frac{1}{C_1} = A_c\Delta x\rho_c c_c + \frac{GA_cc_c\Delta t}{2} + \frac{k_mP_h\Delta x\Delta t A_m\Delta x\rho_m c_m}{L_m(1+k_r)A_m\Delta x\rho_m c_m + k_mP_h\Delta x\Delta t} \tag{42a}$$

$$\frac{1}{C_2} = A_m\Delta x\rho_m c_m + \frac{k_mP_h\Delta x\Delta t}{L_m(1+k_r)} \tag{42b}$$

4.0 Materials Properties and Other Data

CCAN and TCAN contain extensive libraries of materials properties. These are generally stored in two-dimensional arrays and values obtained by linear-linear interpolation.

4.1 Conductor Properties

The present data base is for copper and aluminum conductors. The data consists of the basic zero field properties stored in a 2-D array form for a wide range of temperature and purities, plus correlations for the effect of magnetic fields.

For copper, the thermal conductivity, specific heat and electrical resistivity are accurate over 4 - 600 K and 30 - 3000 RRR, where RRR is Residual Resistance Ratio, η_{273K}/η_{0K}, is a measure of purity [8]. A single median value for density is used throughout this range. Magnetic field effects on electrical resistivity are included using the Kohler equation form

$$\ln\left[\frac{\eta(B,T)-\eta(0,T)}{\eta(0,T)}\right] = -7.00 + 1.383\left[\ln\frac{B\,\eta(0,273K)}{\eta(0,T)}\right] - 0.0298\left[\ln\frac{B\,\eta(0,273K)}{\eta(0,T)}\right]^2 \quad (43)$$

This is a good fit to copper data over 0 to 10 Tesla.

For aluminum, the thermal conductivity, specific heat and electrical resistivity are accurate over 4 - 600 K and 30 - 3000 RRR [8]. A single median value for density is used throughout this range. Magnetic field effects on electrical resistivity are included using the Kohler equation form

$$\frac{\eta(B,T)-\eta(0,T)}{\eta(0,T)} = \frac{0.00177B\,\eta(0,273K)/\eta(0,T)}{1.+0.0005B\,\eta(0,273K)/\eta(0,T)} \quad (44)$$

This is only an approximate fit to aluminum data over 0 to 10 Tesla, which seemed fairly scattered [9,10,11].

There is limited data available on magnetoconductivity, but enough to indicate substantial reductions in thermal conductivity in high purity, low temperature copper and aluminum as magnetic field increases to 8 T or so [8,12]. In order to estimate this effect, note that for pure metals in no magnetic field, $k_m\eta_m \simeq CT$, where $C = 2.45 \times 10^{-8}$ W-Ω/K^2. Since k_m and η_m depend on conduction electrons (not phonons), we assume that magnetic fields decrease thermal and electrical conductivity proportionally. This overestimates the reduction of k_m, especially in strong fields, since phonon heat conduction provides a lower limit to thermal conductivity. The final scaling equation used is

$$\frac{k_m(B,T)}{k_m(0,T)} = 0.2 + 0.8\frac{\eta_m(0,T)}{\eta_m(B,T)} \quad (45)$$

The magnetic field effect on resistivity is obtained from Eqns.(43) and (44). For alloys, thermal conduction depends strongly on phonons so magnetoconductivity effects are small.

4.2 Coolant Properties

Gaseous helium, liquid nitrogen and liquid water properties are included as functions of temperature and pressure [16]. Magnetic field effects are assumed negligible.

For all coolants, the needed properties are specific heat, viscosity, thermal conductivity and density. The data ranges are 6 - 600 K and 0.1 to 15 MPa for gHe; 65 - 125 K and 0.1 - 15 MPa for ℓN_2; and 273 - 613 K, 0.1 - 15 MPa for ℓH_2O. Note that the N_2 data includes the critical point (126.2 K, 3.396 MPa) and data (especially specific heat) should be considered only approximate near these conditions. Saturation pressure correlations are needed for ℓN_2 and ℓH_2O to determine the onset of boiling, and are expressed as

$$p_{sat}(\ell N_2) = 9.473 \times 10^8 \exp(-707.4/T) \tag{46a}$$

$$p_{sat}(\ell H_2O) = 5.157 \times 10^{-5}(T - 255.2)^{4.484} \tag{46b}$$

Both viscosity and saturation pressures are evaluated at film temperature - half-way between the coolant bulk temperature and the wall surface temperature.

For all coolants, the compressibility K_c and expansivity β_c are defined in Eqns.(20) and (21), and are obtained by estimating the derivatives of ρ_c from the $\rho_c(P, T_c)$ data. The Joule-Thompson coefficient ψ_c represents an interesting property and is treated somewhat differently. In general, it is the isenthalpic change of temperature with pressure and is negative, indicating heating with pressure drop. However for helium gas (and others such as H_2 and Ne), the potential energy of intermolecular attraction can increase as pressure drops, resulting in a drop in gas temperature. For helium, this occurs in a range of (T,P) roughly bounded by (40 K, 0 MPa), (20 K, 2 MPa) and (0 K, 0 MPa). This effect may be useful in cryogenic gHe-cooled systems where a sufficient pressure drop per unit length may supply enough $-\Delta T$ from the Joule-Thompson effect to counter the $+\Delta T$ picked up the the helium coolant, resulting in a very uniform temperature along the cooled length. This effect is not important for ℓN_2 or ℓH_2O, so ψ_c is only crudely estimated from β_c as given by Eqn.(23). However, since it may be a significant or desired contribution in cryogenic gHe systems, enthalpy values for helium from 6 - 600 K and 0.1 - 15 MPa are

supplied and ψ_c estimated as $\psi_c = -(\partial h_c/\partial p)_T/c_c$. If more accuracy is needed, values of ψ_c should be provided directly.

5.0 Sample Runs and Validation

5.1 Water-cooled copper conductors – steady-state

Anaconda Copper published a technical report [13] that describes their hollow copper conductors and provides engineering diagrams relating current, coolant velocity, coolant temperature rise and coolant pressure drop. Three cases were selected and analyzed using both CCAN and TCAN (run until steady-state reached). The results are in Table 2. The calculated values were obtained by interpolating on the Anaconda report charts as well as from standard correlations.

5.2 Transient cooldown

According to heat conduction theory, if a body is suddenly immersed in a coolant at a temperature T_{c0}, with surface heat transfer coefficient h and negligible internal temperature gradients ($k_m A_m/hV_m > 6$), then [2],

$$\frac{q'''V_m/hA_m - T_m + T_{c0}}{q'''V_m/hA_m - T_{m0} + T_{c0}} = \exp\left[\frac{-A_m ht}{V_m \rho_m c_m}\right] \tag{47}$$

where q''' is internal heat rate; $V_m/A_m = A_m/P_h$ is the volume-to-surface-area ratio for axially cooled conductors; and T_{m0} is initial conductor temperature.

Figure 1 compares this theory with TCAN calculations for a thin internally-cooled copper conductor in ℓN_2 ($k_m A_m/hV_m \approx 100$). The differences become larger with time because property values change slightly in TCAN while only constant initial values were used in the theoretical curve.

5.3 Long cryogenic gHe cooled tubes

In an experimental simulation of a superconducting power transmission line cooled by 10 K gHe, a long ($L/D \approx 10^5$) copper cable was studied to determine steady-state performance [14]. The three cases reported provide a good test of the compressible flow features, including the Joule-Thompson effect. The overall parameters are 0.181 cm^2 flow area, 300-500 m long tubes wrapped in a large drum with 22 m/turn, and heat leaks of 0.06 to 0.09 W/m. Figure 2 shows the experimental and calculated results.

Case 1 was a straightforward, relatively incompressible case, and agreed reasonably with CCAN and TCAN. Cases 2 and 3 involved compressible flow where CCAN is more appropriate. Here, CCAN matched the experimental results well, but required 10-20 % higher mass flows than measured (which were somewhat uncertain themselves).

5.4 Instabilities with cryogenic gHe

Cryogenic gas cooled electric current leads are used to supply power to superconducting magnets. A flow instatility related to rapid variation of properties with temperature, particularly viscosity, can result in loss of cooling. Here, experimental and theoretical predictions [15] are compared with CCAN results. The "hot" and "cold" leads are modelled separately as internally-cooled, horizontal copper conductors at about 6 K and 0.1 MPa. The cold lead was 0.66 m long, with A_m = 0.135 cm^2; A_c = 0.20 cm^2; P_h = 1.3 cm, P_w = 3.352 cm; and 0.326 W/lead heat leak. The "hot" lead had wider flow passages so was less susceptible to the flow instability.

Figure 3 shows the reported results and CCAN predictions. Onset ot the instability was indicated by lack of convergence and/or rapidly escalating temperatures. Two differences between CCAN and the reported results were the 6 K used in CCAN versus the 4 K in the experiments (CCAN property correlations only go down to 6 K), and the neglection of axial thermal conduction in CCAN. These do not seem to be critical since agreement is good. Four runs with TCAN also agreed with the stability boundary as shown, although an exact threshold is difficult to pin down with TCAN because computer time gets large as the boundary is approached.

6.0 Input/Output

The input variables for CCAN and TCAN are almost identical, and are described in Table 1 with code specific differences marked. Namelist input format is used, so input data can be free-formatted in random order. Sample inputs are shown in Appendix A. Note that the programs are currently inclined towards, but not exclusive for, spiral wound pancake-type magnets.

The output file contains: an input data listing; initial inlet property data; numerical results at different space and time points; final exit property data; and computational time. In CCAN, coolant, interface and maximum conductor temperature data, pressure and

Reynold number profiles are provided at axial points. In TCAN, similar axial temperature data, exit pressure, exit Reynolds number and power consumption are given at time points. In addition, TCAN can plot conductor temperature at the inlet, middle and exit. The plot time points are the same as the print time points. Note that the plot arrays are of limited size - about 300 time points are currently stored.

A description of how to compile, load and execute is provided at the start of each program's source listing. CCAN and TCAN are currently available on the NMFECC CDC 7600 machine, using CHATR to compile (ignore the warning messages), DISSLIB and TV80LIB for plotting, FORTLIB for file linking and utilities, INCAN for the input files, and OCAN and OTAN for output files.

Both CCAN and TCAN have internal error control and convergence parameters that are preset to reasonable values in DATA statements at the start of the main program. CCAN limits the number of iterations ($NMAX = 30$) at each axial step, unless satisfactory convergence ($EPS = 0.001$ %) is achieved on magnet temperature. TCAN chooses a time step based on a fraction ($ADT = 0.1$) of the smaller of: 1) the time between points in the input current/internal heating/coolant temperature data; 2) the time for the coolant to traverse an axial node; and 3) the conductor heat transfer time constant ($A_m \rho_m c_m / P_h h$).

7.0 Conclusions

CCAN and TCAN are reasonably fast, versatile codes for the thermal-hydraulic analysis of many non-superconducting actively-cooled conductors. These programs have been used to analyze ISX-B, TEXTOR and ALCATOR-C bundle divertor designs, TARA mirror coils, and FED copper magnet inserts. Both CCAN and TCAN are available from the authors on the NMFECC CDC 7600 computer.

8.0 References

[1] R.T.Lahey, Jr. and F.J.Moody, "The Thermal Hydraulics of A Boiling Water Nuclear Reactor", American Nuclear Society, Illinois 1977.

[2] W.Rohsenow and H.Choi,"Heat, Mass and Momentum Transfer", Prentice-Hall, Inc., New Jersey 1961.

[3] M.Cerza and W.Reddan, "Description of Computer Program TACC (Thermal Analysis of Copper Conductors)", EP-M-1442, Princeton Plasma Physics Lab, January 27 1977.

[4] J.Schultz, "Cycle Design for a Cryogenic Refrigeration System for FED with Forced Flow Superfluid Helium through Internally Cooled Conductors", PFC/RR-81-29, MIT Plasma Fusion Center, 1981.

[5] M.Hoffman et al, "Review of Heat Transfer Problems Associated with Magnetically Confined Fusion Reactor Concepts", AIChE Symposium Series, 168, Vol.73, 9 (1977).

[6] T.R.Stobridge, "Cryogenic Refrigerators – An Updated Survey", National Bureau of Standards, NBS-TN-655, June 1974.

[7] F.Holland and F.Chapman, "Pumping of Liquids", Reinhold Publ. Corp., New York 1966.

[8] Handbook on Materials for Superconducting Machinery, MCIC-HB-04, Battelle-Columbus Labs, January 1977

[9] R.J.Corruccini, "The Electrical Properties of Aluminum for Cryogenic Electromagnets", National Bureau of Standards, NBS-TN-218.

[10] E.Rocofyllou and C.Papathanassopoulos, "The Magnetoresistance Dependence on Temperature in Al, Al-Ga, Al-Zn, Cu and Cu-Au", Physica 100B, 99 (1980).

[11] M.Snodgrass, F.Blatt, J.Opsal and C.Chiang, "Temperature-Dependent Magnetoresistance of Pure Aluminum and Dilute Al-Ga and Al-Mg Alloys", Phys. Rev. B, 13(2), 574 (1976).

[12] L.L.Sparks, "Magnetic Field Effect on Thermal Conductivity of Selected Metals", p.224, Adv. in Cryog. Eng., 24, K.Timmerhaus, R.Reed and A.Clark (eds.), Plenum Press, New York 1978.

[13] Anaconda Hollow Copper Conductors, Technical Report-56, June 1968.

[14] J.Dean, W.Stewart and J.Hoffer, "Temperature Profiles in a Long Gaseous-Helium-

Cooled Tube", p.250, Adv. in Cryog. Eng., 23, K.Timmerhaus (ed.), Plenum Press, New York, 1977.

[15] P.Thullen, R.Stecher Jr. and A.Bejan, "Flow Instabilities in Gas-Cooled Cryogenic Current Leads", IEEE Trans. on Magnetics, MAG-11 (2), 573 (March 1975).

[16] N.B.Vargaftik, "Tables on the Thermophysical Properties of Liquids and Gases", 2nd ed., Hemisphere Publishing Corp., Washington 1975.

APPENDIX A: SAMPLE RUNS

Sample inputs and outputs from validation runs described in Section 5 are listed here to indicate format. The CCAN sample is Case 2 of Section 5.3, a long cryogenic *gHe* cooled tube. This case required 0.26 s of computer time. The TCAN sample is from Case 1 of Section 5.1, a water-cooled copper conductor starting at room temperature. This case required 97 s of computer time to analyze 150 s of real time.

Sample CCAN Input

```
iname="heli" "um c" "oole" "d tr" "ansm" "issi" "on l" "ine " "test"
nodes=300  nturns=23  im=1  ic=1  iprn=20  ncoils=1
axm=0.50e-4 axc=0.181e-4  pw=0.  ph=0.  length=21.92  costh=0.
mdot=0.0033  bmag=0.  rrr=100.  pin=1.0e+6  effp=1.  effr=0.25
tci=9.5
qint=1240.
amps=0.   $
```

Sample TCAN Input

```
iname=" ***" " ana" "cond" "a cu" "-h2o" " cod" "e te" "st a" "3 **"
nodes=31  nturns=1 im=1 ic=3 iprn=15  ncoils=1 mn=3  ncycle=1
axm=0.01 axc=0. ph=0. pw=0.1571  length=18.3  costh=1.0e-8
mdot=10.  bmag=0.  rrr=100.  pin=0.30e7  effp=0.7  effr=0.25  tmi=280.
hist=0. 1. 150.
amps=0. 50000. 50000.
tci=280. 280. 280.
qint=0. 0. 0.
dtp1=2.0  dtp2=50.  dtbrk=4.  tplon=0.  tpron=0.
he=0.  width=0.  rmax=0.     $
```

Sample CCAN Output

```
 ccan(1982) compressible flow analysis:
helium cooled transmission line test
 total mass flow (kg/s) =  0.00330  mass flux/coil (kg/m2-s) =  182.320
 inlet pressure (mpa) =  1.00       inlet temperature (k) =   9.5
 current area (cm2) =    0.50       flow area (cm2) =  0.18
 heated perimeter (cm) =  1.508     wetted perimeter (cm) =  1.508
 magnet current (ka) =   0.         magnet current density (ka/cm2) =  0.
 length/turn (m) =  21.92           number coils =   1
 number turns =  23                 effective coil radius (m) =  3.49
 cosine(angle from vertical) = 0.    number nodes =   300
 conductor (1=cu,2=al) =   1         coolant (1=he,2=ln2,3=water) =  1
 refrigerator efficiency (%) =  25.0 pump efficiency (%) = 100.0
 internal heating (mw/m3) =  0.0012  field strength (tesla) =  0.

 coolant properties at     9.5 k;   1.00 mpa
 cp (j/kg-k) = 7271.88          rho (kg/m3) =   70.15
 mu (kg/m-s) =   0.320e-05      k (w/m-k) =   0.024
 compressibility d(rho)/d(p)*1/rho (1/pa) =  4.712e-07
 expansitivity -d(rho)/d(t)*1/rho (1/k) =  2.462e-01
 joule-thompson coefficient -d(h)/d(p)*1/cp (k/pa) =  1.991e-07
 saturation pressure psat (mpa) =   0.

magnet properties at     9.5 k
 k (w/m-k) =   1.445e+03       resistivity (ohm-m) =   1.570e-10
 residual resistance ratio (res273/res0) =   100.
```

node	z (m)	tcavg (k)	tmin (k)	tmag (k)	tmout (k)	p (mpa)	qvmag (mw/m3)	re
20	34.5	9.54	9.54	9.54	9.54	0.97	0.001	276744.
40	68.1	9.58	9.58	9.58	9.58	0.95	0.001	279995.
60	101.7	9.61	9.61	9.61	9.61	0.92	0.001	283319.
80	135.3	9.65	9.65	9.65	9.65	0.89	0.001	286726.
100	168.9	9.68	9.68	9.68	9.68	0.86	0.001	290232.
120	202.5	9.70	9.70	9.70	9.70	0.83	0.001	293851.
140	236.1	9.73	9.73	9.73	9.73	0.80	0.001	297604.
160	269.7	9.75	9.75	9.75	9.75	0.77	0.001	301517.
180	303.3	9.77	9.77	9.77	9.77	0.73	0.001	305623.
200	336.9	9.78	9.78	9.78	9.78	0.70	0.001	309962.
220	370.6	9.79	9.79	9.79	9.79	0.66	0.001	314589.
240	404.2	9.80	9.80	9.80	9.80	0.62	0.001	319578.
260	437.8	9.80	9.80	9.80	9.80	0.57	0.001	325032.
280	471.4	9.79	9.79	9.79	9.79	0.53	0.001	331095.
300	505.0	9.75	9.76	9.76	9.76	0.48	0.001	337916.

magnet power requirements(mw)

total/coil	electrical	pumping	cooling	total sources	exit p(mpa)	t(k)
0.0083	0.	0.0000	0.0082	0.0083	0.0000	0.48	9.8

```
coolant properties at      9.8 k;   0.48 mpa
cp (j/kg-k) = 6719.43          rho (kg/m3) =   31.28

mu (kg/m-s) =   0.259e-05      k (w/m-k) =   0.020
compressibility d(rho)/d(p)*1/rho (1/pa) =  2.506e-06
expansitivity -d(rho)/d(t)*1/rho (1/k) =  3.779e-01
joule-thompson coefficient -d(h)/d(p)*1/cp (k/pa) =  2.968e-06
saturation pressure psat (mpa) =   0.

magnet properties at      9.8 k
k (w/m-k) =   1.483e+03        resistivity (ohm-m) =   1.570e-10
residual resistance ratio (res273/res0) =   100.
exit velocity (m/s) =   5.83
calculational time (s) =   0.2596
```

Sample TCAN Output

```
tcan(1982) time dependent flow analysis:
*** anaconda cu-h2o code test a3 **
total mass flow (kg/s) = 10.00000  mass flux/coil (kg/m2-s) = 5091.637
inlet pressure (mpa) =  3.00       inlet temperature (k) = 280.0
current area (cm2) =  100.00       flow area (cm2) = 19.64
heated perimeter (cm) = 15.710     wetted perimeter (cm) = 15.710
length/turn (m) =  18.30           number turns =   1
effective coil radius (m) =     *
number of nodes =   31            cosine(angle from vertical) = 0.000
number of coils =    1            magnetic field =  0.
pump hydraulic efficiency (%) =  70. refrigerator efficiency (%) =  25.
conductor (1=cu,2=al) =   1         coolant (1=he,2=ln2,3=water) =  3
time controls (s):  tend=  150.0    step=  0.0116
initial print step=  2.00    final print step= 50.00 print step change=   4.00
iprn=   15 mn=    3 nodes=   31 ncycle=    1 time plot on=     0.

coolant properties at t(k)=280.0 p(mpa)=  3.00
kc(w/m-k)= 0.583   rhoc(kg/m**3)=1001.2
cpc(j/kg-k)= 4.198e+03      muc(kg/m-s)= 1.489e-03

magnet properties at t(k)=280.0
km(w/m-k)= 396.9 rhom(kg/m**3)= 8930.
cpm(j/kg-k)= 376.0     resm(ohm-m)= 1.614e-08
res273(ohm-m)= 1.570e-08   rrr=  100.0

  time(s)   current(amps)   inlet temp(k)   int heat source(kw/m**3)
     0.          0.          280.000        0.
     1.000    50000.000      280.000        0.
   150.000    50000.000      280.000        0.
```

```
adjacent nodes for cross-node heat transfer
  1   1      2   2      3   3      4   4      5   5      6   6
  7   7      8   8      9   9     10  10     11  11     12  12
 13  13     14  14     15  15     16  16     17  17     18  18
 19  19     20  20     21  21     22  22     23  23     24  24
 25  25     26  26     27  27     28  28     29  29     30  30
 31  31

time=   0.   sec
   n    tc    ts    tm    n    tc    ts    tm    n    tc    ts    tm
   1 280.0 280.0 280.0  16 280.0 280.0 280.0  31 280.0 280.0 280.0

time=   2.00 sec
   n    tc    ts    tm    n    tc    ts    tm    n    tc    ts    tm
   1 280.0 280.1 280.2  16 280.0 280.1 280.2  31 280.0 280.1 280.2
 exit re=171345.    exit h(kw/m**2-k)=   10.6    current(ka)=  50.00
 total energy added(j)= 9.8e+04
 total energy transferred to coolant (j)= 2.09e+03
 electric power (kw)=   73.9 internal heating (kw) =    0.
 refrigeration power (kw) =   21.4 pumping power (kw)=    1.1
 exit p (mpa)= 2.92

time=   3.99 sec
   n    tc    ts    tm    n    tc    ts    tm    n    tc    ts    tm
   1 280.0 280.3 280.4  16 280.1 280.3 280.4  31 280.1 280.3 280.4
 exit re=171967.    exit h(kw/m**2-k)=   10.7    current(ka)=  50.00
 total energy added(j)= 2.5e+05
 total energy transferred to coolant (j)= 1.18e+04
 electric power (kw)=   74.0 internal heating (kw) =    0.
 refrigeration power (kw) =   21.4 pumping power (kw)=    1.1
 exit p (mpa)= 2.92

time=   5.99 sec
   n    tc    ts    tm    n    tc    ts    tm    n    tc    ts    tm
   1 280.0 280.4 280.6  16 280.1 280.4 280.6  31 280.2 280.5 280.6
 exit re=172618.    exit h(kw/m**2-k)=   10.7    current(ka)=  50.00
 total energy added(j)= 3.9e+05
 total energy transferred to coolant (j)= 2.87e+04
 electric power (kw)=   74.0 internal heating (kw) =    0.
 refrigeration power (kw) =   21.4 pumping power (kw)=    1.1
 exit p (mpa)= 2.92

time=  55.99 sec
   n    tc    ts    tm    n    tc    ts    tm    n    tc    ts    tm
   1 280.0 282.1 283.1  16 280.7 282.6 283.5  31 281.4 283.0 283.9
 exit re=182957.    exit h(kw/m**2-k)=   11.0    current(ka)=  50.00
 total energy added(j)= 4.1e+06
 total energy transferred to coolant (j)= 1.97e+06
 electric power (kw)=   74.9 internal heating (kw) =    0.
 refrigeration power (kw) =   20.9 pumping power (kw)=    1.1
 exit p (mpa)= 2.92
```

```
time= 106.00 sec
   n    tc    ts    tm    n    tc    ts    tm    n    tc    ts    tm
    1 280.1 282.4 283.6  16 280.9 283.1 284.3  31 281.7 283.8 284.9
 exit re=186410.    exit h(kw/m**2-k)=   11.0    current(ka)=  50.00
 total energy added(j)= 7.9e+06
 total energy transferred to coolant (j)= 5.25e+06
 electric power (kw)=   75.1 internal heating (kw) =    0.
 refrigeration power (kw) =   20.8 pumping power (kw)=    1.1
 exit p (mpa)= 2.92

time= 150.00 sec
   n    tc    ts    tm    n    tc    ts    tm    n    tc    ts    tm
    1 280.1 282.4 283.6  16 280.9 283.3 284.4  31 281.8 284.1 285.2
 exit re=187357.    exit h(kw/m**2-k)=   11.1    current(ka)=  50.00
 total energy added(j)= 1.1e+07
 total energy transferred to coolant (j)= 8.44e+06
 electric power (kw)=   75.1 internal heating (kw) =    0.
 refrigeration power (kw) =   20.8 pumping power (kw)=    1.1
 exit p (mpa)= 2.92

 coolant properties at t(k)=281.7 p(mpa)=  2.92
 kc(w/m-k)= 0.586   rhoc(kg/m**3)=1001.0
 cpc(j/kg-k)= 4.197e+03      muc(kg/m-s)= 1.359e-03

 magnet properties at t(k)=285.2
 km(w/m-k)= 396.8 rhom(kg/m**3)= 8930.
 cpm(j/kg-k)= 376.8     resm(ohm-m)= 1.647e-08
 res273(ohm-m)= 1.570e-08   rrr=  100.0

 calculational time (s) =  97.1140
```

Sample TCAN Plot

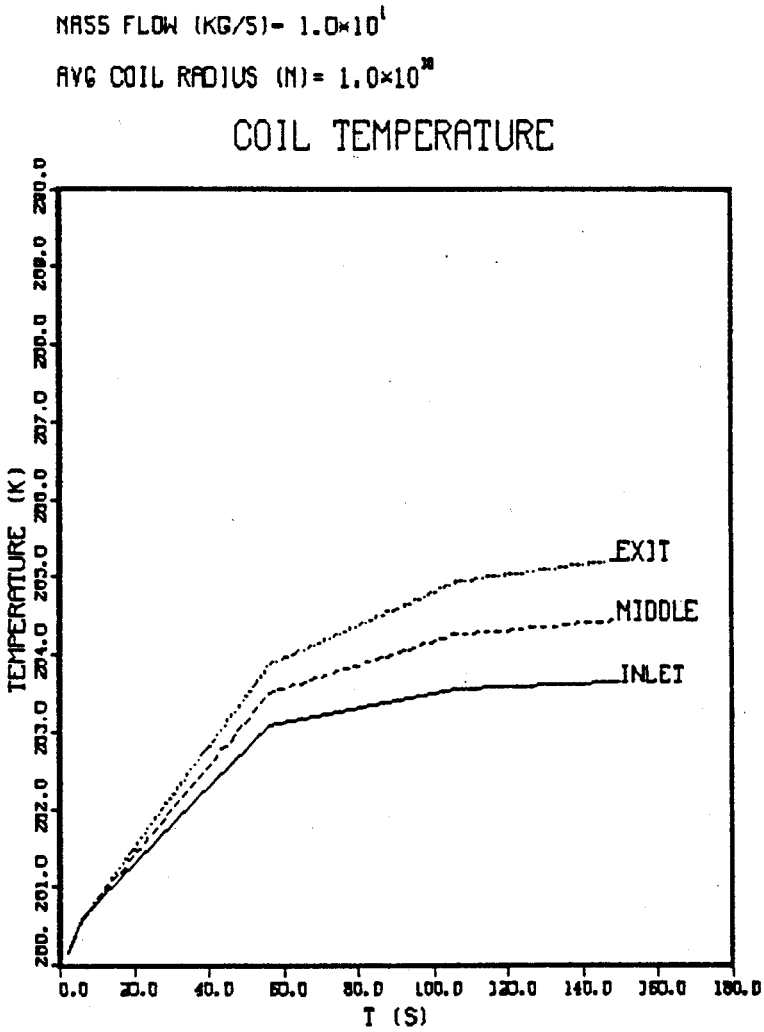

Table 1: Input Variables for CCAN and TCAN

Variable	Unit	Description
INAME		80 character title for printout
NODES		Number of axial nodes (max 300)
NTURNS		Number of conductor turns (1 if single length)
IM		Conductor material: 1/2 = copper/aluminum
IC		Coolant material: 1/2/3 = $gHe/\ell N_2/\ell H_2O$
IPRN		Temperature printout control: every IPRN'th axial node
NCOILS		Number of conductor coils
AXM	m^2	Conductor cross-sectional area
AXC	m^2	Coolant cross-sectional area Total magnet cross-sectional area is AXM + AXC plus support and insulation for each turn.
PH	m	Heated perimeter
PW	m	Wetted perimeter If any of AXC, PH or PW are zero, the program assumes a circular channel with area AXC, or perimeter PW, or perimeter PH (in that order) and calculates the remaining dimensions.
LENGTH	m	Length of one conductor turn
COSTH		Cosine of angle from vertical; for example, COSTH = −1 indicates vertical flow downwards; COSTH = 0 is a special case and indicates a spiral wound coil with no net height change, COSTH arbitrarily small but non-zero indicates straight and horizontal coil.
MDOT	kg/s	Mass flow rate per coil
BMAG	Tesla	Magnetic field in conductor
RRR		Residual Resistance Ratio η_{0K}/η_{273K}
PIN	Pa	Inlet pressure
EFFP		Fractional pump hydraulic efficiency
EFFR		Fractional refrigerator non-Carnot efficiency

Table 1 (continued): Input Format for CCAN and TCAN

Variable	Unit	Description
		Current/Tempurature/q'''/Time information is given at a set of time points. Values at intermediate points are obtained by linear interpolation.
AMPS(I)	Amps	Conductor current through AXM at HIST(I)
TCI(I)	K	Coolant inlet temperature at HIST(I)
QINT(I)	W/m^3	Non-ohmic internal heating at HIST(I)
HIST(I)	s	Time*(Only needed for TCAN)*
		(Only needed for TCAN)
MN		Number of time points in input time/temp/current profile
NCYCLES		Number of time cycles to follow
TMI	K	Magnet initial temperature
		(Only needed for TCAN)
		Output is only provided at user-chosen breakpoints
DTP1	s	Initial time breakpoint step size
DTP2	s	Final time breakpoint step size
DTBRK	s	Time for change from DTP1 to DTP2
TPLON	s	Time to turn on plotter
TPRON	s	Time to turn on printout
		(Only needed for TCAN)
		This data is only needed for cross-coil heat transfer. Code currently has crude algorithm that determines the nearest axial node in adjacent pancake for the double pancake design with inlet near outlet (as in ISX-B and TARA coils).
HE	W/m^2-K	Effective cross-coil heat transfer coefficient; HE = 0 indicates no cross-coil heat transfer.
WIDTH	m	Width of conductor
RMAX	m	Outer radius of pancake coil

Table 2: Steady-state water-cooled copper test

	CASE 1	CASE 2	CASE 3
INPUT:			
L (m)	18.3	5.	18.3
A_m (cm^2)	1.	1.	100.
D (cm)	0.5	0.5	5.
$T_{c,inlet}$ (K)	280.	280.	280.
p_{inlet} (MPa)	5.	5.	3.
I (kA)	1.	10.	50.
GA_c (kg/s)	0.1	0.4	10.
RESULTS:	CCAN/TCAN/Empirical	CCAN/TCAN/Empirical	CCAN/TCAN/Empirical
$T_{c,exit}$ (K)	287/287/289	338/338/330	282/282/282
$T_{m,exit}$ (K)	288/288/	357/359/	284/285/
Re	21200/21000/21000	231000/236000/	185000/188000/186000
Δp (MPa)	1.27/1.28/1.22	3.54/3.50/4.5	0.08/0.08/0.08
P_{elec} (kW)	3.0/3.0/	96/96/	75/75/
P_{pump} (kW)	0.1/0.1/	1.4/1.4/	0.77/0.77/

Note: Square conductor cross-section; internal circular coolant channel; 100 RRR copper; no magnetic field; 100% pump hydraulic efficiency.

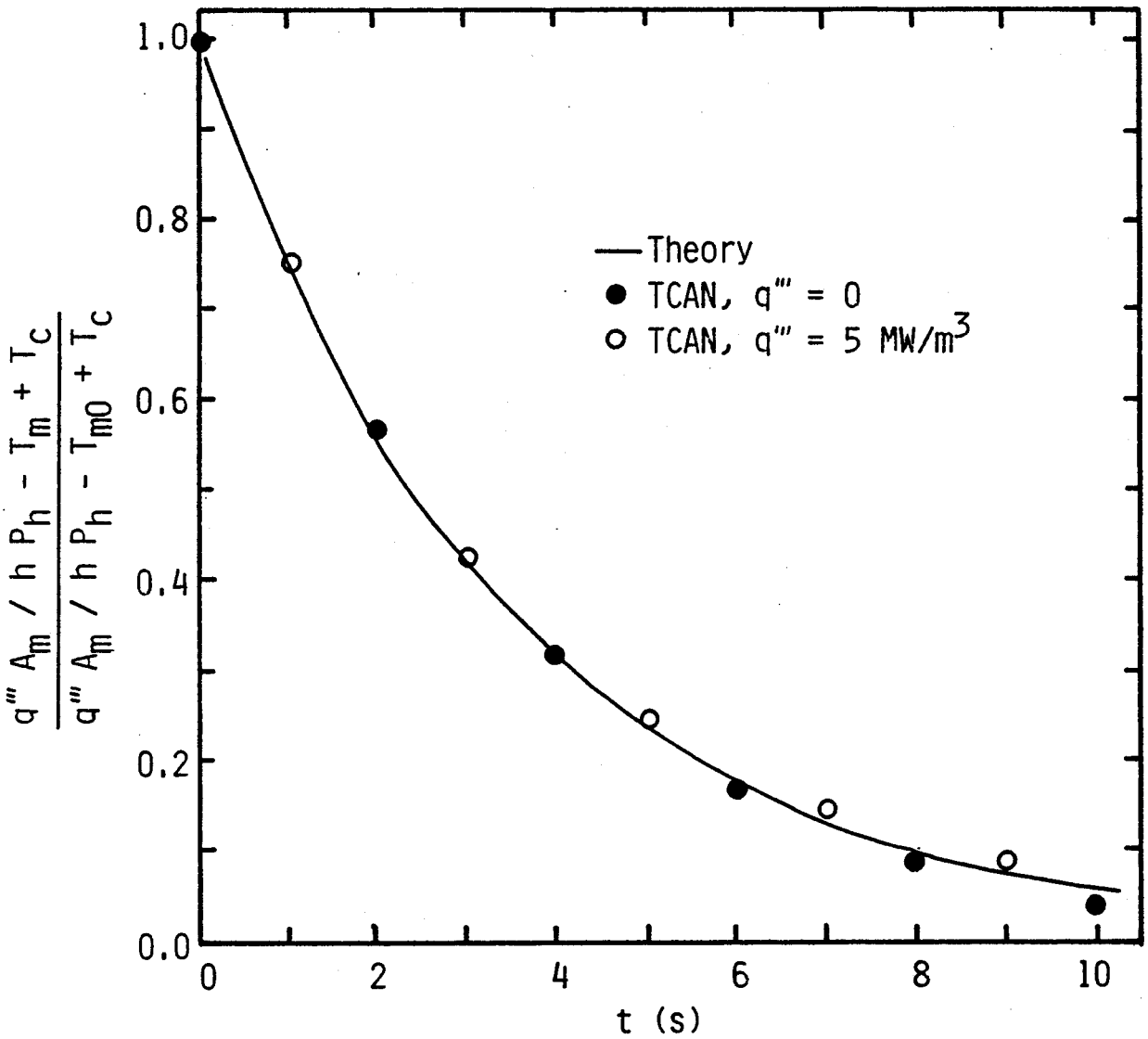

Figure 1: Transient cooldown of a thin body, initially at T_{m0}, placed in coolant at fixed temperature T_c. Parameters: A_m = 1 cm^2; P_h = 3.5 cm; $h \simeq$ 1700 W/m^2·K; T_c = 70 K; and T_{m0} = 110 K.

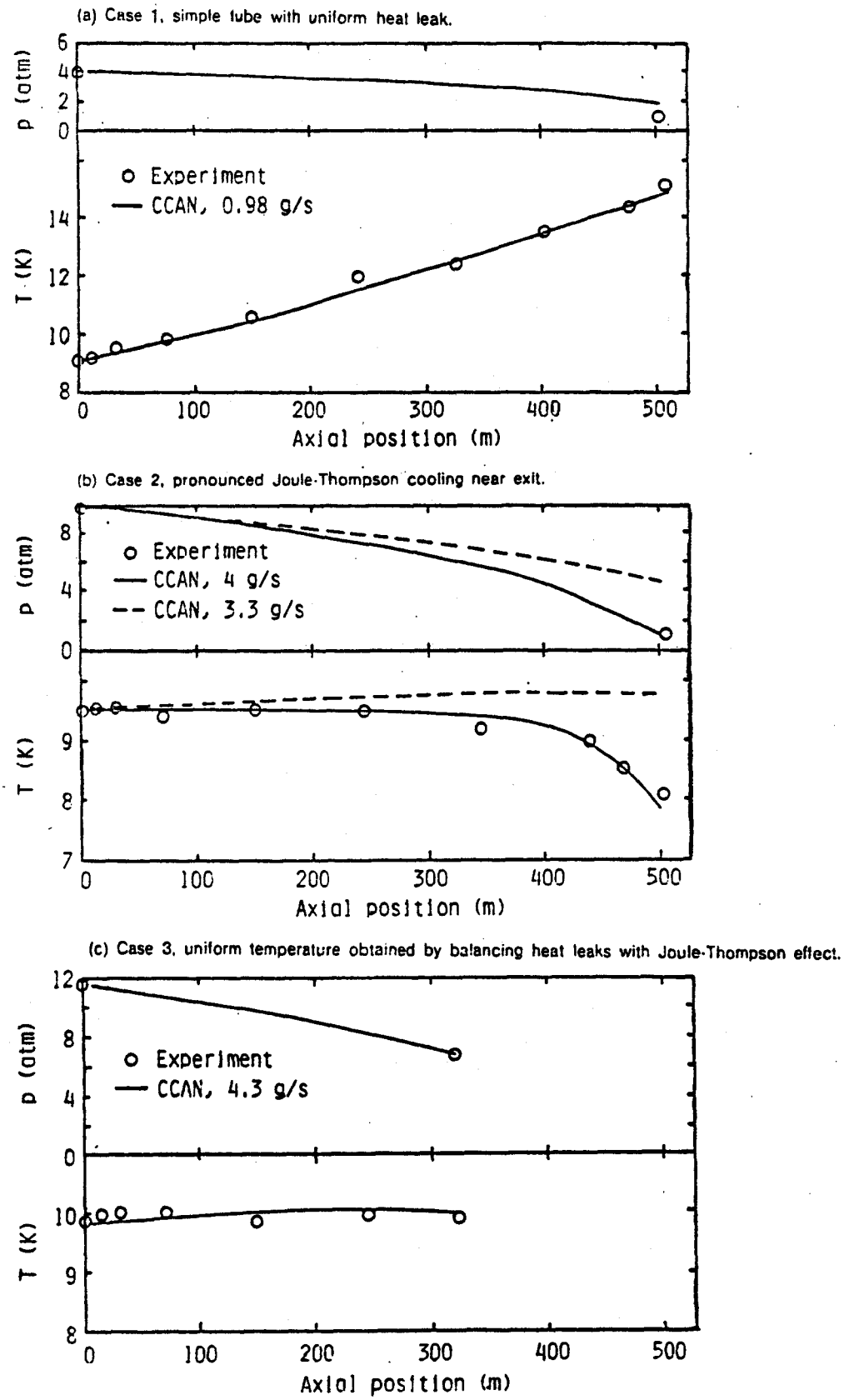

Figure 2: Long cryogenic *gHe* cooled tubes at different inlet conditions.

DISTRIBUTION BEYOND UC20:

PFC BASE MAILING LIST

Argonne National Laboratory, TIS, Reports Section
Associazione EURATOM - CNEN Fusione, Italy, The Librarian
Battelle-Pacific Northwest Laboratory, Technical Info Center
Brookhaven National Laboratory, Research Library
Central Research Institute for Physics, Hungary, Preprint Library
Chinese Academy of Sciences, China, The Library
The Flinders University of S.A., Australia, Jones, Prof. I.R.
General Atomic Co., Library
General Atomic Co., Overskei, Dr. D.
International Atomic Energy Agency, Austria,
Israel Atomic Energy Commission, Soreq Nucl. Res. Ctr., Israel
Kernforschungsanlage Julich, FRG, Zentralbibliothek
Kyushu University, Japan, Library
Lawrence Berkeley Laboratory, Library
Lawrence Livermore Laborary, Technical Info Center
Max-Planck-Institut fur Plasma Physik, FRG, Main Library
Nagoya University, Institute of Plasma Physics, Japan
Oak Ridge National Laboratory, Fusion Energy Div. Library
Oak Ridge National Laboratory, Derby, Roger
Physical Research Laboratory, India, Sen, Dr. Abhijit
Princeton University, PPL Library
Rensselaer Polytechnic Institute, Plasma Dynamics Lab.
South African Atomic Energy Board, S. Africa, Hayzen, Dr. A.
UKAEA, Culham Laboratory, United Kingdom, Librarian
US Department of Energy, DOE Library
Universite de Montreal, Lab. de Physique dés Plasmas, Canada
University of Innsbruck, Inst. of Theoretical Physics, Austria
University of Saskatchewan, Plasma Physics Lab., Canada
University of Sydney, Wills Plasma Physics Dept., Australia
University of Texas at Austin, Fusion Res. Ctr., Library
University of Wisconsin, Nucl. Eng. Dept., UW Fusion Library

INTERNAL MAILINGS

MIT Libraries
Industrial Liaison Office
G. Bekefi, A. Bers, D. Cohn, B. Coppi, R.C. Davidson,
T. Dupree, S. Foner, J. Freidberg, M.O. Hoenig, M. Kazimi,
L. Lidsky, E. Marmar, J. McCune, J. Meyer, D.B. Montgomery,
J. Moses, D. Pappas, R.R. Parker, N.T. Pierce, P. Politzer,
M. Porkolab, R. Post, H. Praddaude, D. Rose, J.C. Rose,
R.M. Rose, B.B. Schwartz, L.D. Smullin, R. Temkin, P. Wolff,
T-F. Yang

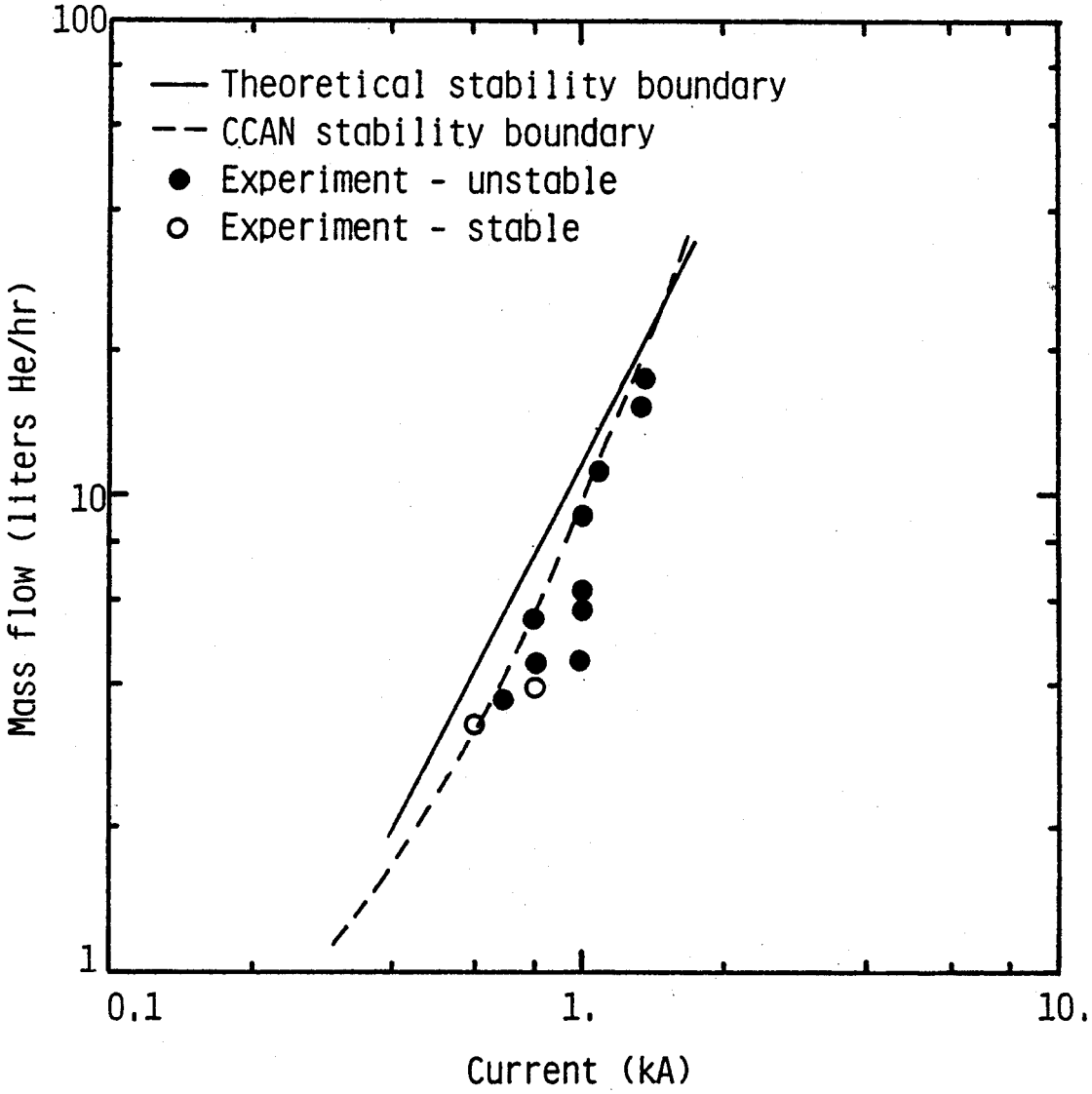

Figure 3: Cryogenic flow instability in *gHe* cooled current leads.